Functional divergence of the *bag of marbles* gene in the *Drosophila melanogaster* species group

Jaclyn E. Bubnell[1*], Cynthia K.S. Ulbing[1], Paula Fernandez Begne[1], and Charles F. Aquadro[1*]

[1] Department of Molecular Biology and Genetics, Cornell University, Ithaca, NY, USA

*Correspondence: Jaclyn Bubnell, jeb486@cornell.edu and Charles Aquadro, cfa1@cornell.edu

Authors performed the following: JEB - conceptualization, investigation, validation, formal analysis, and writing. CKSU and PFB - investigation, and validation, CFA - conceptualization, funding acquisition, supervision, and writing.

Abstract

In *Drosophila melanogaster,* a key germline stem cell (GSC) differentiation factor, *bag of marbles* (*bam*) shows rapid bursts of amino acid fixations between sibling species *D. melanogaster* and *D. simulans*, but not in the outgroup species *D. ananassae*. Here, we test the null hypothesis that *bam'*s differentiation function is conserved between *D. melanogaster* and four additional *Drosophila* species in the *melanogaster* species group spanning approximately 30 million years of divergence. Surprisingly, we demonstrate that *bam* is not necessary for oogenesis or spermatogenesis in *D. teissieri* nor is *bam* necessary for spermatogenesis in *D. ananassae*. Remarkably *bam* function may change on a relatively short time scale. We further report tests of neutral sequence evolution at *bam* in additional species of *Drosophila* and find a positive, but not perfect, correlation between evidence for positive selection at *bam* and its essential role in GSC regulation and fertility for both males and females. Further characterization of *bam* function in more divergent lineages will be necessary to distinguish between *bam's* critical gametogenesis role being newly derived in *D. melanogaster*, *D. simulans*, *D. yakuba,* and *D. ananassae* females or it being basal to the genus and subsequently lost in numerous lineages.

Introduction

In most sexually reproducing animals, egg and sperm production begins with the differentiation of germline stem cells. These germline stem cells (GSCs) divide both to self-renew to maintain the germline and to produce daughter cells that differentiate to produce gametes (Kahney et al. 2019). The cellular processes of daughter cell differentiation and stem cell self-renewal are the most fundamental functions of stem cells and are therefore highly regulated and presumed to be conserved. In the germline, the mis-regulation of either of these processes leads to sterility (Gleason et al. 2018). However, many of the genes that control GSC maintenance and GSC daughter differentiation in *D. melanogaster* are rapidly evolving due to positive selection for amino acid diversification (Civetta et al. 2006; Bauer DuMont et al. 2007; Choi and Aquadro 2015; Flores, DuMont, et al. 2015).

One such gene is *bag-of-marbles* (*bam*) which exhibits a rapid burst of amino acid substitutions between the sister species *D. melanogaster* and *D. simulans*, acts as the key switch for GSC daughter cell differentiation in *D. melanogaster* females, and is necessary for terminal differentiation of spermatogonia in males (McKearin and Spradling 1990; Civetta et al. 2006; Bauer DuMont et al. 2007; Insco et al. 2009). Despite 60 fixed amino acid differences between *D. melanogaster* and *D. simulans,* a *D. simulans bam* transgene is sufficient for GSC daughter cell differentiation in *D. melanogaster* females and males. The intriguing observations that *bam* is both rapidly evolving due to positive selection and functions as a switch for GSC daughter differentiation in *D. melanogaster* has led us to investigate what could be driving its positive selection between species (Flores, Bubnell, et al. 2015).

In females, *bam* is repressed in GSCs, and upon its expression promotes differentiation by binding to the protein product of *benign gonial cell neoplasm* (*bgcn)* as well as a series of other protein partners to repress the translation of self-renewal factors *nanos* and *eIF4a* (Li et al. 2009; Ting 2013). The GSC daughter cell differentiates into a cystoblast, which then goes through four rounds of mitotic divisions while *bam* localizes

to the fusome, a cellular structure that interconnects the resulting dividing cells that make up the cyst. In these cells, Bam functions with Bgcn to regulate mitotic synchrony (Chen and McKearin 2003). Before meiosis begins, *bam* expression is repressed. In males, *bam* is expressed in GSCs and its expression increases as differentiation progresses (Insco et al. 2009). In early dividing spermatogonia, Bam protein must reach a threshold to bind with partners Bgcn and *tumorous testis* (*tut*) to repress *mei-P26* and switch the cellular program from proliferation to terminal differentiation to begin meiosis (Chen et al. 2014). After this switch, *bam* expression is rapidly repressed. Loss of *bam* function in either sex results in the over-proliferation of either GSCs in females or spermatogonia in males causing tumors and sterility (McKearin and Spradling 1990).

One possible explanation for the observed signal of positive selection at *bam* is a change of function. As *bam* regulates gametogenesis, it is possible that life history or environmental factors drive positive selection at *bam*. It is even possible that the genetic interaction between the endosymbiotic bacteria *Wolbachia pipientis* and *bam* has led to such changes in *bam*'s function in different lineages, as *Wolbachia* infects the GSC niche and is propagated through the germline (Flores, Bubnell, et al. 2015). While functional divergence of *bam* seems less likely due to its essential role in GSC maintenance and differentiation in *D. melanogaster, bam* sequence is highly divergent among species. It is even difficult to confidently align *bam* sequence between *D. melanogaster* and *D. ananassae,* both members of the *melanogaster* species group (subgenus Sophophora), let alone the many more divergent *Drosophila* species (Bauer DuMont et al. 2007). Additionally, *bam* appears to be a novel gene in the genus *Drosophila* as no orthologues are reported in any non-*Drosophila* genomes using orthoDB v10 (Kriventseva et al. 2019) and Ensembl Metazoa (Howe et al. 2020) (both accessed 11/4/2021).

Here, we investigate the possibility that the observed signals of positive selection in *D. melanogaster* and *D. simulans* at *bam* are due to selection for a novel function for *bam* in gametogenesis in these lineages. To do this, we ask if *bam* is necessary for gametogenesis in diverse species within the *Drosophila* genus. We generate *bam* loss-

124 of-function alleles in five *Drosophila* species in the *melanogaster* species group (*D.*
125 *melanogaster*, *D. simulans*, *D. yakuba*, *D. teissieri*, and *D. ananassae*). Surprisingly, we
126 find that *bam* is not necessary for gametogenesis in one or both sexes in two species
127 within the *melanogaster* species group. We also analyze additional population samples
128 of species mainly within the *melanogaster* species group and a few more distant
129 lineages for nucleotide sequence variation at *bam.* Within the *melanogaster* species
130 subgroup (*D. melanogaster*, *D. simulans*, *D. yakuba*, *D. santomea*, and *D. teissieri*), we
131 find evidence of lineage-specific signals of adaptation for three species, but not for *D.*
132 *teissieri* or *D. santomea*. Outside of the *melanogaster* species subgroup, we find similar
133 patterns of lineage-specific signals of positive selection. Together with our *bam* loss-of-
134 function results, these observations raise the possibility that the critical role for *bam* in
135 GSC differentiation is newly derived in the *melanogaster* species group and the
136 signatures of positive selection we observe in some of those species is associated with
137 species-specific refinements of *bam*'s GSC differentiation function or species-specific
138 adaptive pressures acting on *bam*'s GSC differentiation function.
139

140 ## Results

141

142 **Generating *bam* null alleles for non-*melanogaster* species**

143 To ask if *bam's* GSC function is conserved in species outside of *D. melanogaster*, we
144 designed and generated a series of *bam* null alleles in five species in the *melanogaster*
145 species group to assay for GSC daughter differentiation (Fig 1A). To do this, we used
146 CRISPR/Cas9 to introduce a 3xP3-YFP or a 3xP3-DsRed gene cassette into the first
147 exon of *bam*, thereby disrupting the *bam* coding sequence and introducing a premature
148 termination codon (Fig 1B). This also generates an allele that is trackable by eye color,
149 which is necessary for the non-*melanogaster* species of which we do not have balancer
150 chromosomes to maintain alleles that cause sterility. To generate the homozygous *bam*
151 null genotype, we cross the 3xP3-YFP line to the 3xP3-DsRed line and select flies with
152 both DsRed and YFP positive eyes. This scheme also allows us to use the same cross
153 to assay the heterozygous and wildtype *bam* siblings (Table 1).
154

155 We used *D. melanogaster* as a control to ensure our method would generate a loss of
156 function *bam* phenotype, as the *bam* null phenotype has been well characterized in this
157 species (Table 1). We also generated *bam* nulls in four other species within the
158 *melanogaster* species group *D. simulans*, *D. yakuba*, *D. teissieri,* and *D. ananassae*
159 (Fig 1A).
160
161 ***bam* is necessary for female and male fertility in *D. melanogaster*, *D. simulans*,**
162 **and *D. yakuba*, but only in *D. ananassae* females, and in neither *D. teissieri* males**
163 **nor females.**
164 In *D. melanogaster*, both male and female *bam* nulls are sterile as early germline cells
165 fail to differentiate and proceed through gametogenesis. In classic null alleles of *D.*
166 *melanogaster bam* ($bam^{\Delta 59}$ and $bam^{\Delta 86}$), one copy of functional *bam* is sufficient to
167 rescue the *bam* null sterility phenotype. We first asked if our novel *bam* null alleles
168 behaved this way in *D. melanogaster*. Heterozygotes of each 3xP3-DsRed or 3xP3-YFP
169 disruption line showed similar fertility to wildtype *bam* in both males and females (mean
170 difference of adult progeny, not significant, permutation test) and transheterozygous
171 males and females carrying both the 3xP3-DsRed and the 3xP3-YFP disruptions (which
172 we will term the *bam* null genotype) were completely sterile (mean difference of adult
173 progeny, $P < 0.0001$, permutation test) (Fig 1 , File S2). We observed this same pattern
174 for *D. simulans* and *D. yakuba* (Fig 1, File S2). We observed some sterile *D. simulans*
175 females and males across all *bam* genotypes, which we attribute to the strain and
176 unlikely to be related to *bam* (Fig 1, File S2). In contrast, in *D. teissieri* we found that
177 there was no difference in fertility between any of the *bam* genotypes tested for females
178 or males (mean difference of adult progeny, not significant, permutation test) (Fig 1, File
179 S2). The *bam* null genotype did not result in sterility, or even reduced fertility. In *D.*
180 *ananassae*, *bam* null females were sterile (mean difference of adult progeny, $P <$
181 0.0001, permutation test), and heterozygotes of each 3xP3-DsRed or 3xP3-YFP
182 disruption did not significantly reduce fertility (mean difference of adult progeny, not
183 significant, permutation test). However, in *D. ananassae* males, *bam* nulls were fertile,
184 with no significant mean difference in progeny across the tested *bam* genotypes (Fig 1,

185 File S2). Therefore, *bam* is not necessary for fertility in all species in the *melanogaster*
186 species group, or even all species within the *melanogaster* species subgroup.
187
188 **Consistent with the fertility results, *bam* is also necessary for germ cell**
189 **differentiation in *D. simulans* and *D. yakuba* females and males, but not in *D.***
190 ***teissieri* males or females, and only *D. ananassae* females.**
191 The ovaries of *D. melanogaster bam* null females feature over-proliferating germline
192 stem cells that fail to differentiate into cystoblasts (McKearin and Spradling 1990; Ting
193 2013). This results in the germarium and developing downstream cysts accumulating
194 small, GSC-like cells resembling tumors (Fig 3A). In the testes of *D. melanogaster bam*
195 null males spermatogonia differentiation is blocked. The resulting testes feature over-
196 proliferating spermatogonia that fail to develop into terminally differentiated
197 spermatocytes (Fig 3A) (Insco et al. 2009; Insco et al. 2012).
198
199 We imaged ovaries from 2-5 day old *D. melanogaster* females from each *bam*
200 genotype. We assayed for the characteristic *bam* null tumor phenotype using antibodies
201 to Vasa to visualize the morphology of the germline and Hts-1B1 to visualize the
202 fusome, which fails to fully form in *bam* mutants (Lavoie et al. 1999; Hinnant et al.
203 2020). We found that the *bam* null genotype resulted in the characteristic *bag of*
204 *marbles* phenotype consistent with classic *bam* null alleles, with tumorous ovaries filled
205 with undifferentiated GSC-like cells (Fig 3B). One copy of wildtype *bam* was sufficient to
206 rescue the *bam* null phenotype, as has been previously observed for other *bam* null
207 alleles (Fig 3B) (Lavoie et al. 1999; Flores, Bubnell, et al. 2015). Therefore, our 3xP3-
208 DsRed and 3xP3-YFP disruptions successfully recapitulate the *bam* null phenotype in
209 females. We imaged testes from 3-5 day old *D. melanogaster* males and also
210 immunostained with antibodies to Vasa to label the germline and Hts-1B1 to label the
211 fusome. We found that the *bam* null genotype resulted in tumorous testes filled with
212 small over-proliferating cells that fail to differentiate into spermatocytes (Fig 3B). We
213 found that one copy of wildtype *bam* was sufficient to rescue the *bam* null tumor
214 phenotype, as has been previously reported for classic *bam* null alleles (Gönczy et al.

1997; Shivdasani and Ingham 2003)(Fig 3B). Therefore, our *bam* null alleles also recapitulate the previously described *bam* null phenotype in *D. melanogaster* males.

We repeated the same analysis for the other species in the study. We found for *D. simulans* and *D. yakuba* both female and male homozygous *bam* null genotypes exhibited the characteristic ovarian and testes tumors as described in *D. melanogaster* (Fig 3B). In these two species for both males and females, one copy of *bam* was also sufficient to rescue the *bam* null phenotype as observed in *D. melanogaster* (Fig 3B). However, in the *D. teissieri bam* null genotype, we observed no evidence of GSC over-proliferation in females or spermatogonia over-proliferation in males. We observe the same phenotype for the heterozygous alleles in both males and females, as well as wildtype (Fig 3B). This indicates that *bam* is not necessary for GSC daughter differentiation in *D. teissieri* females nor is *bam* necessary for spermatogonia differentiation in males. In *D. ananassae bam* null females, we observed the characteristic *bam* null phenotype observed in *D. melanogaster* with over-proliferating GSC-like cells in the germarium and cysts and undeveloped fusomes (Fig 3B). One copy of *bam* was sufficient to rescue the *bam* null tumorous phenotype (Fig 3B). Therefore the *D. ananassae* female *bam* null phenotype is consistent with that of *D. melanogaster*, *D. simulans*, and *D. yakuba*. In contrast, in *D. ananassae* males of the *bam* null genotype we did not observe over-proliferating spermatogonia (Fig 3B). The homozygous *bam* null genotype resulted in the same phenotype as the heterozygous bam null genotypes and wildtype indicating that *bam* is not necessary for the switch from proliferating spermatogonia to differentiated spermatocytes in *D. ananassae* males. Therefore, these cytological data are fully consistent with our fertility assay observations.

Confirming the loss-of-function status of *bam* in the *bam* null disruption design

The only available Bam antibody is weakly cross-reactive in *D. melanogaster* and *D. simulans* thus we cannot directly demonstrate the absence of Bam protein in all the species tested (Flores 2013; Flores, Bubnell, et al. 2015). Although we used the same design to generate the *bam* null alleles across this study and therefore expect the 3xP3-

246 DsRed and 3xP3-YFP disruptions to have the same effect on *bam* in all five species, we
247 further confirmed the loss-of-function status of the *bam* disruption alleles in *D.*
248 *ananassae* and *D. teissieri* given their functional divergence.
249
250 First, we asked if *bam* had undergone duplication events in *D. ananassae* and *D.*
251 *teissieri* using publicly available sequence data and found no evidence of *bam*
252 duplication in either species (details described in S1 File, S8 Table). Next, since the
253 3xP3-DsRed and 3xP3-YFP insertions introduce a premature termination codon, we
254 expect the mRNA of the disrupted *bam* allele to be degraded through nonsense
255 mediated mRNA decay (NMD), but if the premature termination codon induced exon
256 skipping, the disrupted *bam* exon could be alternatively spliced out resulting in
257 expression of a truncated *bam* allele, which may be sufficient for function (Brogna and
258 Wen 2009; Mou et al. 2017; Chen et al. 2018; Sui et al. 2018). We used RT-qPCR to
259 ask if patterns of expression in the *bam* null alleles in *D. ananassae* males and *D.*
260 *teissieri* females and males were consistent with expectations for NMD. We found that
261 for *D. ananassae* and *D. teissieri*, the expression of the *bam* null disruption alleles were
262 reduced relative to the *bam* wildtype allele to levels consistent with NMD (~1-50%,
263 details in S1 File, Fig S1. Fig S2) (Pereverzev et al. 2015). Therefore, the mRNA of the
264 *bam* disruption alleles are likely targeted for degradation. Additionally, since both *bam*
265 null *D. teissieri* males and females show wildtype phenotypes we looked for evidence of
266 exon skipping. We asked if the exon disrupted by 3xP3-YFP or 3xP3-DsRed in the *bam*
267 null genotypes was expressed in proportion to the non-disrupted exons relative to the
268 wildtype genotype. We found that the ratio of exon 1 to exon 2 expression was not
269 significantly different between *D. teissieri* nulls and *D. teissieri* wildtype genotypes for
270 males and females (details in S1 File, Fig S3).
271
272 Although *bam* null *D. ananassae* males and *D. teissieri* males and females exhibited
273 wildtype phenotypes, together the genomic and RT-qPCR analyses indicate that the
274 *bam* null alleles are loss-of-function alleles. This evidence therefore supports our
275 conclusion that *bam* is not required for spermatogenesis in *D. ananassae* and *D.*
276 *teissieri* nor oogenesis in *D. teissieri.*

277

278 ***D. ananassae bam* null males show evidence of germline defects**

279 In *D. melanogaster*, Fas3 expression in the testes is limited to the hub, the testes
280 microenvironment that houses the somatic and germline stem cell populations at the
281 apical tip of the testes. As we found that *bam* was necessary for oogenesis in *D.*
282 *ananassae* but not for spermatogenesis, we assayed for more subtle evidence of
283 germline defects in *D. ananassae* males. We immunostained testes with an antibody to
284 Fas3 to look for evidence of ectopic expression of Fas3 as in Gonzalez et al. (Gonzalez
285 et al. 2015). In *D. melanogaster bam* null males, Fas3 is ectopically expressed, as the
286 spermatogonia over proliferate (Fig 4A&B). In *D. ananassae bam* null males, we also
287 observed ectopic expression of Fas3 in cells outside of the apical tip of the testes,
288 although not nearly as severe as in *D. melanogaster bam* null males (Fig 4D&E). We
289 then asked if there was any evidence of ectopic Fas3 expression in *D. teissieri bam* null
290 males, as we also found that *bam* was not necessary for spermatogenesis in *D.*
291 *teissieri.* In contrast to *D. ananassae* and *D. melanogaster,* we did not observe ectopic
292 expression of Fas3 in *D. teissieri bam* null males (Fig 4B&C). This indicates that while
293 *bam* is not necessary for differentiation in *D. ananassae* males, it may be playing a role
294 in regulating the early differentiating germ cell population.

295

296 ***bam* shows lineage-specific bursts of positive selection throughout the**
297 ***Drosophila* genus.**

298 Previous studies have reported that *bam* is evolving under strong positive selection
299 detected by the McDonald-Kreitman test in *D. melanogaster* and *D. simulans*, but not in
300 *D. ananassae* (Civetta et al. 2006; Bauer DuMont et al. 2007; Choi and Aquadro 2014).
301 As these three species span about 30 million years of divergence, we wanted to know if
302 there was evidence of positive selection in lineages more closely related to *D.*
303 *melanogaster* and *D. simulans*, or if this signal was unique to the individual *D.*
304 *melanogaster* and *D. simulans* lineages. We expanded the species sampled to include
305 three closely related species from the *yakuba* complex: *D. yakuba, D. santomea,* and *D.*
306 *teissieri*. We also took advantage of published population genomic data from samples of
307 inbred lines to expand our assessment of *bam* variation in additional population

308 samples for *D. melanogaster* (Lack et al. 2015) and *D. simulans* and to newly assess
309 *bam* variation in population samples in the *montium* species group (*D. serrata, D.*
310 *bunnanda, D. birchii,* and *D. jambulina*) and the *ananassae* species subgroup (*D.*
311 *bipectinata, D. pseudoananassae,* and *D. pandora*) (Li et al. 2021).
312
313 In addition to further sampling closely related species to *D. melanogaster* and *D.*
314 *simulans,* we also wanted to ask if there was any evidence of adaptive evolution at *bam*
315 in lineages outside of the *melanogaster* group. We resequenced *bam* from population
316 samples of three more distantly related *Drosophila* species: *D. pseudoobscura*, *D.*
317 *affinis*, and *D. mojavensis* which span approximately 70 million years of divergence (Li
318 et al. 2021). We also used published population genomic data from samples of inbred
319 lines to assess *bam* variation in *D. immigrans* and *D. rubida*, both members of the
320 *immigrans* species group (Li et al. 2021).
321
322 To ask if any population samples showed departures from selective neutrality consistent
323 with positive selection at *bam* similar to what we previously observed for *D.*
324 *melanogaster* and *D. simulans*, we used a lineage-specific McDonald-Kreitman test
325 (MKT) (Siddiq et al. 2017). The null hypothesis of the MKT is that the ratio of
326 nonsynonymous to synonymous polymorphism within a species is equal to the ratio of
327 nonsynonymous to synonymous fixed differences between species (or in our case, a
328 predicted common ancestral sequence). A previous study reported signatures of
329 positive selection at *bam* as an excess of nonsynonymous fixations in the *D.*
330 *melanogaster* and *D. simulans* lineages (Bauer DuMont et al. 2007). As *bam* appears to
331 be experiencing episodic signals of adaptive evolution restricted to individual lineages,
332 we measured lineage-specific divergence. We used codeml to generate reconstructed
333 ancestral sequences at the node of interest by maximum likelihood (Yang 1997; Yang
334 2007). We then used this sequence to calculate nonsynonymous and synonymous
335 divergences for each population sample. We excluded polymorphisms below 12% as
336 low-frequency mutations are likely to be slightly deleterious and reduce the power of the
337 MKT to identify positive selection (Fay et al. 2002; Charlesworth and Eyre-Walker
338 2008).

339

340 For *D. melanogaster*, we utilized the Zambia population sample from the *Drosophila*
341 genome Nexus to measure *bam* variation (Lack et al. 2015). The Zambia sample
342 contains the largest sample size of intact *bam* sequence (few missing calls), and
343 represents variation found in the ancestral range of *D. melanogaster*. We used the
344 predicted common ancestor of *D. melanogaster* and *D. simulans* and found similar
345 patterns of polymorphism and divergence to the smaller samples of *D. melanogaster*
346 from the USA and Zimbabwe previously reported by Bauer DuMont et al. (Bauer
347 DuMont et al. 2007) (Fig 5). The *D. melanogaster* lineage shows a strong signal of
348 positive selection (alpha = 0.943, P=0.001) (Fig 5).
349

350 For *D. simulans bam*, we utilized the Burnley, Victoria population sample from Li et al.
351 (Li et al. 2021). We used the same common ancestral sequence as we did for the *D.*
352 *melanogaster* analysis to calculate divergence. The *D. simulans* lineage shows a signal
353 of positive selection for *bam* (alpha=0.722, P=0.036) are consistent with those
354 previously reported by Bauer DuMont et al. (Bauer DuMont et al. 2007) (Fig 5). We also
355 assessed *bam* variation in the *D. simulans* CA, USA population sample from Signor et
356 al. (Signor et al. 2018), but due to elevated levels of genome-wide intermediate
357 frequency polymorphisms caused by a recent population bottleneck, this sample
358 violates key assumptions for the McDonald-Kreitman test (Fay 2011; Messer and Petrov
359 2013). For completeness, we report our findings for the CA sample in Supplementary
360 File S1.
361

362 We used the predicted common ancestor of the *yakuba* complex (*D. yakuba*, *D.*
363 *santomea*, *D. teissieri*) to estimate divergence for *bam* in each of the population
364 samples. For *D. yakuba* we also observed a significant signal of positive selection for
365 *bam* (alpha=0.893, P=0.002) (Fig 5). In contrast, we could not reject neutrality for *D.*
366 *teissieri bam* or for *D. santomea bam.* The estimate of alpha is very low for *D. teissieri*
367 (alpha=-0.011, P=0.983), but for *D. santomea* the alpha value was high, although not
368 significant (alpha=0.76, P=0.186), which suggests it may be informative to sample *bam*
369 from additional *D. santomea* populations with larger sample sizes (n=11 here) (Fig 5).

370

371 In the *montium* species subgroup, we used the predicted common ancestor of *D.*
372 *serrata, D. bunnanda, D. birchii,* and *D. jambulina* to calculate divergence for *bam.* We
373 found a significant signal of positive selection for *bam* in *D. serrata* (alpha=0.799,
374 P=0.003)*, D. birchii* (alpha=0.675, P=0.003)*,* and *D. jambulina* (alpha=0.618, P=0.023)
375 (Fig 5)*.* However, we could not reject neutrality for *D. bunnanda* (alpha=-1.014,
376 P=0.542) (Fig 5).
377

378 In the *ananassae* species group, we used the predicted common ancestor of *D.*
379 *bipectinata, D. pseudoananassae, D. pandora,* and *D. ananassae* to calculate
380 divergence for *bam.* We reassessed lineage-specific divergence at *bam* for the *D.*
381 *ananassae* population sample previously reported by Choi et al (Choi and Aquadro
382 2014) as they reported divergence between *D. ananassae* and *D. atripex*. We did not
383 reject neutrality at *bam* for *D. bipectinata* (alpha=0.355, P=0.357)*, D. pseudoananassae*
384 (alpha=-0.866, P=0.613)*,* or *D. pandora* (alpha=0.666, P=0.11) (Fig 5)*.* However, we
385 found a significant signal of positive selection for *bam* in *D. ananassae* (alpha=1,
386 P=0.045) (Fig 5). Therefore, the signals of positive selection at *bam* previously reported
387 for *D. melanogaster* and *D. simulans* are not unique to the *melanogaster* species group.
388

389 In the *obscura* species group, we calculated divergence for *bam* from population
390 samples of *D. pseudoobscura* and *D. affinis* from their predicted common ancestor and
391 observed similar patterns of polymorphism and divergence (*D. pseudoobscura*:
392 alpha=0.487, P=0.448), (*D. affinis*: alpha=-1.064, P=0.349), neither of which were close
393 to rejecting neutral expectations (Fig 5). We used the predicted common ancestor of *D.*
394 *mojavensis* and *D. arizonae bam* to calculate divergence in the *D. mojavensis* lineage
395 and again did not observe a trend towards an excess of nonsynonymous divergence
396 (alpha=0.285, P=0.771) (Fig 5). For the *immigrans* species group, we calculated
397 divergence for *bam* from the predicted common ancestor of *D. immigrans* and *D. rubida,*
398 We did not reject neutrality for *bam* in *D. immigrans* (alpha=0.116, P=0.882), but we did
399 find a strong signal of positive selection for *bam* in *D. rubida* (alpha=1, P<0.000) (Fig 5).

400 Therefore, the signals of positive selection at *bam* are heterogeneously distributed
401 throughout the *Drosophila* genus.
402
403
404 ## Discussion
405 **Bam's role in germline stem cell maintenance and differentiation shows**
406 **remarkable variation in the *Drosophila melanogaster* species group.**
407 Our comparative assessment of *bam* requirement in gametogenesis across diverse
408 *Drosophila* species indicates that the functional evolution of *bam* is unexpectedly
409 complex. We discovered that *D. teissieri* and *D. ananassae* do not require *bam* for
410 gametogenesis in one or both sexes. A single orthologous copy of *bam* is found in all
411 *Drosophila* species examined to date, but is absent in outgroups for example, house fly
412 (Musca) and the sheep blow fly (Lucinia). These results raise the question as to whether
413 *bam*'s critical role in GSC differentiation originally characterized in *D. melanogaster* is in
414 fact a phylogenetically recent gain of function, or whether *bam*'s critical role is basal to
415 the genus and that *bam*'s role has been recently (and possibly repeatedly) lost in
416 specific lineages. For example, assuming *bam*'s role in GSC differentiation is basal,
417 then the most parsimonious explanation of our functional data is that *bam* was required
418 for oogenesis and spermatogenesis in the common ancestor of the species tested (Fig
419 1A), then *bam* function was lost in *D. ananassae* males, and then lost again
420 independently in *D. teissieri* males and females. These alternative scenarios can be
421 distinguished by future follow-up analyses of *bam* function in more divergent *Drosophila*
422 species.
423
424 **Evidence of positive selection for protein diversification at Bam is strikingly**
425 **heterogeneous across divergent *Drosophila* lineages.**
426 We analyzed additional population samples of species mainly within the *melanogaster*
427 species group and a few more distant lineages for nucleotide sequence variation at
428 *bam.* We found new evidence of lineage-specific signals positive selection for
429 accelerated protein sequence evolution at *bam* in three of the *melanogaster* subgroup
430 species (*D. melanogaster, D. simulans*, and *D. yakuba*), three of the *montium* subgroup

species (*D. serrata, D. birchii,* and *D. jambulina*), and one of the *ananassae* subgroup species (*D. ananassae*). Additionally, we found evidence of positive selection in the *D. rubida* lineage, indicating that the protein diversification at *bam* is repeatedly occurring in species spanning over 70 million years of divergence.

While we could not reject neutrality for *bam* for the remaining lineages, It is important to note as well that the MKT has limited power statistically when applied to single genes (Akashi 1999; Zhai et al. 2009) and thus a failure to reject selective neutrality does not prove that positive selection is not acting or has not acted on this gene.

Are stem cell genes hotspots for adaptive evolution?

The results of past studies of GSC evolution (Bauer DuMont et al. 2007; Choi and Aquadro 2014; Choi and Aquadro 2015; Flores, DuMont, et al. 2015) and our population genetic and functional results in this study lead to the question of why GSC developmental functions are frequent targets of adaptation. It has been documented that selfish transposable elements are upregulated in the absence of piRNAs, implying that piRNAs act to protect the germline genome leading to an evolutionary conflict that may drive positive selection at piRNA genes (Aravin et al. 2007; Simkin et al. 2013). There is natural variation in the gene *Bruno* that provides tolerance to deleterious P-element expression in the genome (Kelleher et al. 2018). In a scRNA-seq study of male *D. melanogaster* testes, Witt et al. (Witt et al. 2019) report many fixed de novo genes expressed in GSCs and early spermatogonia (where *bam* is expressed) at similar levels to testis-specific genes. In contrast, segregating de novo genes show lower expression in GSCs and early spermatogonia implying that cell type expression may impact the likelihood for a de novo gene to become fixed. As de novo gene evolution is increasingly recognized as a critical mode of adaptation, especially in reproduction, GSCs/early spermatogonia may be generating necessary variation for adaptation (Witt et al. 2019). A recent finding that the insect gene *oskar,* which is critical for germ cell formation and oogenesis, arose *de novo* through a horizontal gene transfer event from a prokaryote, resulting in a fusion between prokaryotic and eukaryotic sequence

462 illustrates yet another mechanism by which novel genes can take on key developmental
463 roles in reproduction (Jenny et al. 2006; Blondel et al. 2020).
464
465 The *bam* sequence itself has many properties of novel genes: it does not contain any
466 known DNA or RNA binding motifs, it binds with multiple protein partners, contains
467 structurally disordered regions, and is expressed in a tight spatiotemporal manner
468 (Chen et al. 2010; Jiang and Assis 2017; Wilson et al. 2017; Klasberg et al. 2018;
469 Vakirlis and McLysaght 2019). Novel genes that become fixed often gain critical roles in
470 conserved gene networks. Their new role may lead to selection to fine tune their critical
471 role thereby providing additional functional flexibility for these conserved processes
472 (Chen et al. 2010). Such a process could represent what has been called
473 developmental systems drift, a model to explain how developmental systems remain
474 phenotypically conserved while the genetic pathways that determine them diverge (True
475 and Haag 2001).
476
477 It is possible that *bam* was a gene novel to the common ancestor of *Drosophila* (and
478 possibly some other dipterans) and has functionally diversified across the *Drosophila*
479 genus, only gaining its role in germline stem cell differentiation in the lineage leading to
480 the *melanogaster* species group. Additionally, it is possible that *bam* quickly evolved a
481 role in GSC daughter differentiation in *Drosophila,* but that function has been shaped by
482 germline conflicts in specific lineages. Conflict with germline agents (such as *W.*
483 *pipientis)* may even drive the fixation of novel genes in new roles that successfully
484 evade their control. As *W. pipientis* must recognize host cues during oogenesis to
485 successfully infect the developing oocyte, it is possible that novel host genes that
486 regulate differentiation might then be under selection for their new function if it evades
487 unfavorable manipulation by *W. pipientis*.
488
489 It certainly seems plausible that genetic conflict is one way for new genes to evolve
490 required functions in conserved processes such as GSC daughter differentiation. The *D.*
491 *melanogaster* testes and the accessory gland show enriched expression of novel
492 genes, many of which show signals of adaptive evolution, and some of which are

493 predicted to be driven by sexual conflict (Levine et al. 2006; Zhou et al. 2008; Findlay et
494 al. 2009; Kaessmann 2010; Gubala et al. 2017; Witt et al. 2019). While the
495 developmental processes of gametogenesis and reproduction must be conserved, our
496 results demonstrate that the individual genes that function in that process may vary
497 among even closely related species.
498

499 ## Materials and Methods

500

501 **Fly stocks and rearing:**
502 We raised fly stocks on standard cornmeal molasses food at room temperature. We
503 used yeast glucose food for fertility assays. The *D. melanogaster* w^{1118} isogenic line and
504 w^{1118} balancer lines were gifts from Luis Teixeira, and the *D. simulans* w^{501} line (stock
505 14021-0251.011), the *D. yakuba* white eyed line (14021-226.03) and the *D. ananassae*
506 reference genome (14024-0371.14) lines are from the Drosophila species stock center
507 (http://blogs.cornell.edu/drosophila/). The *W. pipientis*-free *D. ananassae* line Nou83
508 was a gift from Artyom Kopp. The *D. teissieri* line (*teissieri* syn) was a gift from Daniel
509 Matute (Turissini et al. 2015).
510

511 We tested all lines for *W. pipientis* infection status by qPCR (NEB Luna Universal qPCR
512 kit) using primer sets for *wsp* and *arm* (S1 Table). Lines that tested positive (*D. teissieri*,
513 *D. ananassae*, *D. simulans*) were treated with tetracycline (200 µg/mL) for three
514 generations to remove *W. pipientis* (Glover et al. 1990). We allowed these lines to
515 recover for at least three generations before using them in any analyses. We were
516 unable to fully clear the *D. ananassae* reference line of *W. pipientis* with tetracycline, so
517 to obtain a *W. pipientis* free stock, we crossed males of our *bam* null lines to females
518 from the Nou83 line, which we confirmed to be *W. pipientis*-free by qPCR.
519

520 **Cloning for bam null constructs**:
521 We used Flybase to obtain the nucleotide sequence information for designing
522 constructs in *D. melanogaster* (Dmel 5.57)*, D. simulans* (dsim r2.01), *D. yakuba* (dyak
523 r1.04), and *D. ananassae* (dana r1.04) (Thurmond et al. 2019). We obtained sequence

524 information for the *D. teissieri* sequence from Turissini et al. 2017 (accession
525 SAMN07407364-SAMN07407376) (Turissini and Matute 2017). We used Geneious for
526 all cloning design.
527
528 We used the NEB Q5 High Fidelity 2X master mix to generate all PCR products. We gel
529 extracted and purified PCR products using the NEB Monarch DNA gel extraction kit or
530 Qiagen MinElute gel extraction kit. IDT primers were used for PCR, sequencing, and
531 cloning. We generated the donor plasmids for the 3xP3-DsRed and 3xP3-YFP bam
532 disruption lines using the NEB HiFi Assembly Cloning kit into the pHD-attP-DsRed
533 vector from flyCRISPR (Gratz et al. 2014) as follows: we amplified 1.5 kb homology
534 arms from genomic DNA of the appropriate species stock flanking the insertion site for
535 3xP3-DsRed or 3xP3-YFP. 3xP3-DsRed was amplified from the pHD-attP-DsRed
536 plasmid and 3xP3-YFP was amplified from the *D. simulans* nos-Cas9 line, a gift from
537 David Stern. We then gel extracted the two homology arms and the appropriate 3xP3
538 marker, purified them, and assembled them into the pHD vector backbone using the
539 manufacturer's protocol (S3 Table).
540
541 We used the U6:3 plasmid from CRISPRflydesign (Port et al. 2014) to express gRNAs
542 for generating the *D. yakuba* lines. The gRNA target sequence was generated by
543 annealing primers with the gRNA sequence and BbsI site overhangs, and ligating into
544 the BbsI ligated U6:3 vector (T4 ligase NEB, BbsI NEB) (S3 Table). We used NEBalpha
545 competent cells for transformations.
546
547 We prepped and purified all plasmids for embryo injections with the Qiagen plasmid
548 plus midi-prep kit. We additionally purified plasmids for injections with phenol-chloroform
549 extraction to remove residual RNases. We confirmed plasmid sequences with Sanger
550 sequencing (Cornell BRC Genomics Facility).
551
552 **CRISPR/Cas9:**
553 <u>gRNA selection</u>:

554 We chose gRNAs using the flyCRISPR target finder (Gratz et al. 2014) for *D.*
555 *melanogaster*, *D. simulans*, *D. yakuba*, and *D. ananassae*. For *D. teissieri*, we used one
556 completely conserved gRNA from *D. yakuba.* We also chose an additional gRNA from
557 *D. yakuba* that had two divergent sites between *D. yakuba* and *D. teissieri,* thus we
558 modified them to the *D. teissieri* sites. We selected gRNAs that had no predicted off-
559 targets in the reference genome (S4 Table & S5 Table). For *D. yakuba*, we used the
560 U6:3 gRNA plasmid from CRISPRfly design as described above. For the remaining
561 species (*D. melanogaster*, *D. simulans*, *D. teissieri*, and *D. ananassae*), we used
562 synthetic gRNAs (sgRNAs) from Synthego. We used 1-3 gRNAs per injection to
563 increase the chances of a successful CRISPR event. We used multiple gRNAs if there
564 were suitable options for that site to increase efficiency (multiple gRNAs within 50 bps
565 with 0 predicted off-targets).
566
567 Injections:
568 All CRISPR/Cas9 injections were carried out by Genetivision. Lines were injected with
569 the plasmid donor, gRNAs (synthetic or plasmid), Cas9 protein (Synthego), and an
570 siRNA for Lig4 (IDT DNA). The same siRNA was used for *D. melanogaster*, *D.*
571 *simulans*, *D. yakuba*, and *D. teissieri* (pers communication with Daniel Barbash and
572 David Stern S6 Table). We created a *D. ananassae*-specific siRNA due to sequence
573 divergence (S6 Table).
574
575 For the *bam* disruption lines, we screened for eye color in F1s in-house using a
576 Nightsea fluorescence system with YFP (cyan) and DsRed (green) filters. We
577 backcrossed all CRISPR/Cas9 mutants to the stock line we used for injections for three
578 generations. All mutants are maintained as heterozygous stocks. We confirmed all
579 CRISPR insertions by Sanger sequencing (Cornell BRC Genomics Core Facility).
580
581 Genotypes for generating bam disruption homozygotes:
582 We generated two *bam* disruption lines in each species in order to create the genotypes
583 for the comparative *bam* null analyses. We generated one by disrupting *bam* with 3xP3-
584 DsRed and the other with 3xP3-YFP. We selected DsRed or YFP positive flies and

585 crossed them to generate homozygous *bam* disruption flies (*bam*$^{3xp3\text{-}DsRed}$/*bam*$^{3xP3\text{-}YFP}$).
586 This cross also results in DsRed or YFP positive heterozygous *bam* null progeny as well
587 as *bam* wildtype progeny without any fluorescent eye marker.
588
589 We targeted the 1st exon of *bam* in all species in order to disrupt the *bam* coding
590 sequence and introduce an early stop codon. While we were successful in generating
591 1st exon disruptions in each species, in *D. simulans* we were only able to obtain a 3xP3-
592 YFP 1st exon disruption line. However, we did find that a *D. simulans* line with a 3xP3-
593 DsRed insertion in its 2nd intron resulted in homozygous sterile females and males with
594 tumorous ovaries and testes, while heterozygous females and males were fertile with
595 wildtype ovary and testes phenotypes. As this edit was specific to the *bam* locus, we
596 presumed it was an mRNA null allele and we used this line for our analyses. Thus, if the
597 phenotype of the 3xP3-DsRed 2nd intron allele over the 3xP3-YFP 1st exon allele is the
598 same as the homozygous 3xP3-DsRed 2nd intron allele, this is consistent with
599 classification as a genetic null.
600
601 **Fertility assays:**
602 Female fertility:
603 All female fertility assays were performed following the approach of Flores et al. (Flores
604 et al. 2015). Specifically, we collected virgin females and aged them based on their time
605 to sexual maturity 2-3 days (*D. melanogaster*, *D. simulans*, *D. yakuba,* and *D. teissieri*)
606 or 5-7 days (*D. ananassae*) (Markow and O'Grady 2006). We collected all genotypes
607 from each bottle to control for bottle effects. We collected virgin males of the wildtype
608 genotype for each species and aged them for the same timeframe as the females of
609 that species. We evenly distributed males collected from different bottles across the
610 female genotypes to control for any bottle effects. We crossed single females collected
611 within 48 hours of each other to two virgin males. We allowed the trio to mate for 9
612 days, and then flipped them to new vials. Except for *D. ananassae* and *D. yakuba*, as
613 fertility was very low, we cleared the trio after day 9 and did not continue further. For all
614 other species crosses, after an additional 9 days, we cleared the trio. Then, we counted

615 the progeny for each trio every two to three days to get the total adult progeny per
616 female.
617
618 Male fertility:
619 All male fertility assays were performed as described for the female fertility assays
620 except that one tester male was crossed to two virgin females.
621
622 Food and conditions for fertility assays:
623 For *D. melanogaster*, *D. simulans*, *D. ananassae*, and *D. teissieri*, we performed all
624 fertility assays on yeast-glucose food. For *D. yakuba*, we performed fertility assays on
625 cornmeal-molasses food, as this line did not thrive on the yeast-glucose food. We kept
626 all crosses and fertility experiments in an incubator at 25°C with a 12-hour light-dark
627 cycle.
628
629 **Statistics**:
630 For the fertility assays we used estimation statistics to assess the mean difference
631 (effect size) of adult progeny between the wildtype *bam* genotype and each individual
632 additional *bam* genotype. For generating the estimation statistics and plots (Ho et al.
633 2019), we used the dabest package in Python (v. 0.3.1) with 5,000 bootstrap resamples.
634 Estimation statistics provide a non-parametric alternative to other statistical tests of the
635 difference of the mean (for example, ANOVA), and allow us to understand the
636 magnitude of the effect of *bam* genotype on the fertility phenotype. In text, we report
637 significance as a mean difference (effect size) outside the 95% bootstrap confidence
638 interval. While one benefit of these statistics is that they are less biased than reporting
639 traditional P-values, we also report P-values for approximate permutation tests with
640 5,000 permutations.
641
642 **Immunostaining:**
643 We used the following primary antibodies, anti-vasa antibody from Santa Cruz
644 biologicals (anti rabbit 1:200), anti-Hts-1B1 from Developmental Studies Hybridoma
645 bank (anti-mouse 1:4 for serum, 1:40 for concentrate item), and anti-Fas3 from DSHB

646 (anti-mouse 1:50). We used the following secondary antibodies: Alexaflour 488, 568
647 (Invitrogen) at 1:500.
648
649 We performed immunostaining as described in Aruna et al. and Flores et al. (Aruna et
650 al. 2009; Flores, Bubnell, et al. 2015). Briefly, we dissected ovaries and testes in ice-
651 cold 1X PBS and pipetted ovaries up and down to improve antibody permeability. We
652 fixed tissues in 4% paraformaldehyde, washed with PBST, blocked in PBTA (Alfa
653 Aesar, with 0.1% Triton X added), and then incubated in the appropriate primary
654 antibody in PBTA overnight. We then washed (PBST), blocked (PBTA), and incubated
655 the tissue in the appropriate secondary antibody for 2 hours, then washed (PBST) and
656 mounted in mounting media with DAPI (Vecta shield or Prolong Glass with NucBlue) for
657 imaging.
658
659 **Confocal Microscopy:**
660 We imaged ovaries and testes on a Zeiss i880 confocal microscope with 405nm, 488
661 nm, and 568 nm laser lines at 40X (Plan-Apochromat 1.4 NA, oil) (Cornell BRC Imaging
662 Core Facility). We analyzed and edited images using Fiji (ImageJ).
663
664 **RNA extraction:**
665 For RT-qPCR experiments we dissected ovaries from 10 one-day old females per
666 biological replicate or testes from 15 one-day old males in ice cold 1x PBS. The tissue
667 was immediately placed in NEB DNA/RNA stabilization buffer, homogenized with a
668 bead homogenizer, and then stored at -80°C until RNA extraction. We used the NEB
669 Total RNA mini-prep kit for all RNA extractions according to the manufacturer's
670 protocol and included the on column DNAse treatment. We assessed RNA
671 concentration and quality with a Qubit 4 fluorometer and a NanoDrop.
672
673 **RT-qPCR:**
674 For all RT-qPCR analyses, we used the Luna One Step RT-qPCR kit from NEB
675 according to the manufacturer's instructions at 10µl total volume in 384 well plates. We

676 used a Viia7 qPCR machine with the appropriate cycle settings as described in the
677 Luna One Step RT-qPCR kit.
678
679 For the analysis of *bam* expression in *D. ananassae*, we used primers to *D. ananassae*
680 *bam* with *D. ananassae Rp49* as a control (S1 Table). To assess the possibility that the
681 *bam* disruption allele induced exon skipping of the disrupted exon 1 in *D. teissieri*, we
682 designed a primer pair that spanned exon 1 to exon 2 and another pair that spanned
683 exon 2 to exon 3 (S1 Table). We used the exon 2 - exon 3 target as the control. For
684 both the *D. teissieri* and *D. ananassae* assays described above, we included a standard
685 curve for each target on every plate at a 1:2 dilution and then used the standard curve
686 method to calculate the relative quantity of *bam* (to either *Rp49* for *D. ananassae* or
687 *bam* exon 2-exon 3 for *D. teissieri*) with the QuantStudio software using the wildtype
688 *bam* genotype as a control for each species.
689
690 For the allele specific analysis in *D. teissieri,* we designed one primer pair specific to
691 the *bam* 3xP3-DsRed and 3xP3-YFP insertion alleles and another primer pair specific
692 to the wildtype allele. We then used these two targets to measure the relative
693 expression of the insertion allele to the wildtype allele in a single heterozygous sample.
694 The primer pair for the *bam* insertion alleles target the sequence between the SV40-
695 polyA tail of the 3xP3-DsRed and 3xP3-YFP insertion and the *bam* sequence
696 downstream of the insertion (S1 Table). The primer pair for the *bam* wildtype allele
697 target *bam* upstream and downstream of the 3xP3-DsRed and 3xP3-YFP insertion,
698 and therefore will not amplify the large insertion allele under RT-qPCR conditions (S1
699 Table). We included a standard curve for each target on every plate at a 1:2 dilution
700 and then used the standard curve method in the QuantStudio software to calculate the
701 Ct and Ct standard error for each target and each sample. We report the relative
702 quantity of the 3xP3-DsRed or 3xP3-YFP allele using the wildtype allele in the same
703 sample as a control by calculating $2^{-(nullCt-wildtypeCt)}$.
704
705 **Genomic analysis of *bam* copy number in *D. teissieri:***

706 While *bam* is reported as a 1:1 syntenic ortholog on FlyBase for *D. melanogaster, D.*
707 *simulans, D. yakuba,* and *D. ananassae,* data for *D. teissieri* is not available. To ask if
708 *bam* has been recently duplicated in *D. teissieri,* we generated a blast database (blastn
709 v 2.9.0) from a new de novo assembled *D. teissieri* reference genome (accession
710 GCA_016746235.1) and blasted *D. teissieri bam* from the resequencing described
711 above.
712
713 Additionally, to assess read coverage for *bam* compared to the surrounding loci and the
714 entire chromosome 3R, we used publicly available short read WGS data for *D. teissieri*
715 (SRR13202235) and used bwa-mem (v 0.7.17) to map reads to a new de novo
716 assembled *D. yakuba* reference genome (accession GCA_016746365.1). We visualized
717 the alignment and assessed read coverage using Geneious.
718
719 **Population genetic analyses:**
720 The *D. yakuba*, *D. santomea*, and *D. teissieri* population sample lines were gifted by
721 Brandon Cooper and Daniel Matute (Cooper et al. 2017). The *D. yakuba* and *D. teissieri*
722 lines were collected in Bioko in 2013, the *D. santomea* sample was collected in Sao
723 Tome in 2015. The *D. affinis* population sample lines were gifted by Robert Unckless
724 (S2 Table). The *D. mojavensis* population sample is from Organ Pipe National
725 Monument, Arizona and DNA from this sample was gifted by Erin Kelleher and Luciano
726 Matzkin. The *D. pseudoobscura* population sample is from Apple Hill, California, as
727 described in (Schaeffer and Miller 1991). We used previously prepared DNA from the *D.*
728 *pseudoobscura* population sample as described in (Schaeffer and Miller 1991).
729
730 We prepared genomic DNA from *D. affinis, D. yakuba*, *D. santomea*, and *D. teissieri*
731 samples using the Qiagen PureGene kit. We used Primer3 to generate primers to
732 amplify *bam* from *D. affinis, D. mojavensis, D. pseudoobscura, D. yakuba*, *D. santomea*,
733 and *D. teissieri* population samples (S7 Table). We used existing polymorphism data
734 (Daniel Matute, personal communication) to generate primers for *D. yakuba*, *D.*
735 *santomea*, and *D. teissieri*. We resequenced *bam* using Sanger sequencing from
736 5'UTR-3'UTR for *D. yakuba*, *D. santomea*, and *D. teissieri* and *bam* exons and introns

737 for *D. affinis* (Cornell BRC Genomics Facility). We used Geneious for aligning the
738 sequences and calling polymorphisms. We generated fasta files for each individual. We
739 used DnaSP to phase individuals with heterozygous sites, and then randomly picked
740 one allele for further analyses (Bauer DuMont et al. 2007). We will deposit all
741 resequencing data described here in Genbank.
742
743 We used polymorphism data for *D. melanogaster* from the Zambia population sample
744 from the Drosophila genome Nexus (Lack et al. 2015), as this is the largest population
745 sample with intact *bam* sequence and represents a population in the *D. melanogaster*
746 ancestral range. For the *D. melanogaster* Zambia population sample, we removed a
747 single individual that contained missing nucleotide calls in the *bam* coding sequence
748 (ZI117). As we filtered polymorphisms at < 12% frequency, omitting this single individual
749 would not affect our downstream analyses.
750
751 Polymorphism for *D. simulans*, *D. serrata*, *D. bunnanda*, *D. birchii*, *D. jambulina*, *D.*
752 *bipectinata*, *D. pseudoananassae, D. pandora*, *D. immigrans*, and *D. rubida* as well as
753 the single *bam* sequence for *Z. bogoriensis* that we used as an outgroup
754 are from Li et al 2021(accession PRJNA736147) (Li et al. 2021).
755
756 *D. ananassae bam* polymorphism, and single *D. atripex bam* sequences are from Choi
757 et al. (Choi and Aquadro 2014). We obtained single *bam* sequences for species used
758 for outgroups from FlyBase (*D. erecta*), and Genbank (*D. eugracilis, D. arizonae, D.*
759 *navojoa, D. miranda, D. subobscura).*
760
761 We performed all multiple sequence alignments for the *bam* coding sequences using
762 PRANK (v.170427) with the -codon and -F parameters and using the PRANK generated
763 guide tree. As *bam* is highly divergent across the *Drosophila* genus, we generated
764 multiple sequence alignments only among closely related clusters of species to ensure
765 alignment quality. We generated a multiple sequence alignment of the *melanogaster*
766 subgroup species (*D. melanogaster, D. simulans, D. yakuba, D. santomea, D. teissieri,*
767 *D. erecta, D. eugracilis*) and *montium* subgroup species (*D. serrata*, *D. bunnanda*, *D.*

768 *birchii*, *D. jambulina*), a multiple sequence alignment of *D. ananassae, D. bipectinata*, *D.*
769 *pseudoananassae, D. pandora*, and *D. atripex* , a multiple sequence alignment of *D.*
770 *mojavensis, D. arizonae, and D. navajo*, a multiple sequence alignment of *D. affinis, D.*
771 *pseudoobscura, D. miranda,* and *D. subobscura,* and a multiple sequence alignment of
772 *D.immigrans, D. rubida,* and *Z. bogoriensis*.
773
774 We used only unique sequences for input to codeml. We used the codeml package from
775 PAML (v. 4.9) (Yang 1997; Yang 2007) to generate the predicted common ancestor
776 sequences to calculate lineage-specific divergence for *bam* with the McDonald-
777 Kreitman test. We used the PRANK alignments and their corresponding gene trees as
778 input to codeml with the following control file parameters (noisy = 9, verbose = 2,
779 runmode = 0, seqtype = 1, CodonFreq = 2, clock = 0, aaDist = 0, model = 0, NSsites =
780 0, icode = 0, getSE = 0, RateAncestor = 1, Small_Diff = .5e-6, cleandata = 0, method =
781 1).
782
783 We used the http://mkt.uab.cat/mkt/mkt.asp webtool to perform the standard McDonald-
784 Kreitman test (MKT) comparing nonsynonymous vs. synonymous changes (Egea et al.
785 2008). We excluded polymorphic sites at < 12% frequency, as these are likely slightly
786 deleterious alleles that have not yet been purged by purifying selection (Charlesworth
787 and Eyre-Walker 2008). For each species where we had polymorphism data, we
788 performed the MKT using the specified predicted common ancestral sequence to
789 calculate lineage-specific divergence. We report the values of the contingency table, the
790 P-value of the Chi-Square test, as well as alpha, the proportion of fixations predicted to
791 be due to positive selection (Eyre-Walker 2006).
792 **Summary of accession numbers for genomes used in this analysis:**
793 For read coverage analysis of *bam*: *D. teissieri*: SRR13202235, GCA_016746235.1. *D.*
794 *yakuba*: GCA_016746365.1. For cloning *D. teissieri bam* null constructs:
795 SAMN07407364-SAMN07407376. For *bam* polymorphism from *D. simulans, D. serrata,*
796 *D. bunnanda, D. birchii, D. jambulina, D. bipectinata, D. pseudoananassae, D. pandora,*
797 *D. immigrans, and D. rubida*: PRJNA736147.
798

Acknowledgements:

We thank Santiago Herrera Alvarez for resequencing *bam* from *D. affinis* and Jae Young Choi for resequencing *bam* from *D. pseudoobscura* and *D. mojavensis.* We thank Daniel Matute, Brandon Cooper, Robert Unckless, Erin Kelleher, and Luciano Matzkin for the population samples they provided for this study. We thank Fang Li for working to make the variant call files from (Li et al. 2021) quickly available for this study. Additionally, we thank David L. Stern for his advice and guidance in designing the *bam* null alleles and for an extremely thoughtful and critical review of an earlier draft of the manuscript. We are grateful to Mariana F. Wolfner, Andrew G. Clark, Miwa Wenzel and Catherine Kagemann for valuable input and discussion of these experiments and results and helpful comments on this manuscript. Lastly, we thank the three anonymous reviewers for their thoughtful and insightful feedback for improving this manuscript.

Data Availability:

Sequence data generated in this study will be deposited in GenBank prior to publication. The remaining data underlying this article are available in the article and in its online supplementary material. Fly lines, CRISPR/Cas9 reagents, and plasmids used in this study are available upon request.

Funding:

This work was supported by National Institutes of Health grant R01-GM095793 to C.F.A. and by the National Science Foundation Graduate Research Fellowship Program DGE-114415 to J.E.B.

825 REFERENCES

826 Akashi H. 1999. Inferring the fitness effects of DNA mutations from polymorphism and
827 divergence data: Statistical power to detect directional selection under stationarity
828 and free recombination. Genetics. 151(1). doi:10.1093/genetics/151.1.221.
829 Aravin AA, Hannon GJ, Brennecke J. 2007. The Piwi-piRNA pathway provides an
830 adaptive defense in the transposon arms race. Science (80-). 318(5851).
831 doi:10.1126/science.1146484.
832 Aruna S, Flores HA, Barbash DA. 2009. Reduced fertility of Drosophila melanogaster
833 Hybrid male rescue (Hmr) mutant females is partially complemented by Hmr
834 orthologs from sibling species. Genetics. doi:10.1534/genetics.108.100057.
835 Bauer DuMont VL, Flores HA, Wright MH, Aquadro CF. 2007. Recurrent positive
836 selection at Bgcn, a key determinant of germ line differentiation, does not appear to
837 be driven by simple coevolution with its partner protein bam. Mol Biol Evol.
838 24(1):182–191. doi:10.1093/molbev/msl141.
839 Blondel L, Jones TEM, Extavour CG. 2020. Bacterial contribution to genesis of the
840 novel germ line determinant Oskar. Elife. doi:10.7554/eLife.45539.
841 Brogna S, Wen J. 2009. Nonsense-mediated mRNA decay (NMD) mechanisms. Nat
842 Struct Mol Biol. doi:10.1038/nsmb.1550.
843 Charlesworth J, Eyre-Walker A. 2008. The McDonald-Kreitman test and slightly
844 deleterious mutations. Mol Biol Evol. doi:10.1093/molbev/msn005.
845 Chen D, McKearin D. 2003. Dpp Signaling Silences bam Transcription Directly to
846 Establish Asymmetric Divisions of Germline Stem Cells. Curr Biol. 13(20):1786–
847 1791. doi:10.1016/j.cub.2003.09.033.
848 Chen D, Tang JX, Li B, Hou L, Wang X, Kang L. 2018. CRISPR/Cas9-mediated
849 genome editing induces exon skipping by complete or stochastic altering splicing in
850 the migratory locust. BMC Biotechnol. doi:10.1186/s12896-018-0465-7.
851 Chen D, Wu C, Zhao S, Geng Q, Gao Y, Li X, Zhang Y, Wang Z. 2014. Three RNA
852 Binding Proteins Form a Complex to Promote Differentiation of Germline Stem Cell
853 Lineage in Drosophila. PLoS Genet. 10(11):e1004797.
854 doi:10.1371/journal.pgen.1004797.
855 Chen S, Zhang YE, Long M. 2010. New Genes in Drosophila Quickly Become

856 Essential. Science (80-). 330(6011):1682–1685. doi:10.1126/science.1196380.
857 Choi JY, Aquadro CF. 2014. The coevolutionary period of Wolbachia pipientis infecting
858 Drosophila ananassae and its impact on the evolution of the host germline stem
859 cell regulating genes. Mol Biol Evol. doi:10.1093/molbev/msu204.
860 Choi JY, Aquadro CF. 2015. Molecular evolution of drosophila germline stem cell and
861 neural stem cell regulating genes. Genome Biol Evol. 7(11):3097–3114.
862 doi:10.1093/gbe/evv207.
863 Civetta A, Rajakumar SA, Brouwers B, Bacik JP. 2006. Rapid evolution and gene-
864 specific patterns of selection for three genes of spermatogenesis in Drosophila. Mol
865 Biol Evol. 23(3):655–662. doi:10.1093/molbev/msj074.
866 Cooper BS, Ginsberg PS, Turelli M, Matute DR. 2017. Wolbachia in the Drosophila
867 yakuba complex: Pervasive frequency variation and weak cytoplasmic
868 incompatibility, but no apparent effect on reproductive isolation. Genetics.
869 205(1):333–351. doi:10.1534/genetics.116.196238.
870 Egea R, Casillas S, Barbadilla A. 2008. Standard and generalized McDonald-Kreitman
871 test: a website to detect selection by comparing different classes of DNA sites.
872 Nucleic Acids Res. doi:10.1093/nar/gkn337.
873 Eyre-Walker A. 2006. The genomic rate of adaptive evolution. Trends Ecol Evol.
874 doi:10.1016/j.tree.2006.06.015.
875 Fay JC. 2011. Weighing the evidence for adaptation at the molecular level. Trends
876 Genet. 27(9). doi:10.1016/j.tig.2011.06.003.
877 Fay JC, Wyckoff GJ, Wu CI. 2002. Testing the neutral theory of molecular evolution with
878 genomic data from Drosophila. Nature. 415(6875). doi:10.1038/4151024a.
879 Findlay GD, MacCoss MJ, Swanson WJ. 2009. Proteomic discovery of previously
880 unannotated, rapidly evolving seminal fluid genes in Drosophila. Genome Res.
881 19(5):886–896. doi:10.1101/gr.089391.108.
882 Flores HA. 2013. Evolutionary and Functional Analysis of the Drosophila Bag of Marbles
883 Gene. Cornell University.
884 Flores HA, Bubnell JE, Aquadro CF, Barbash DA. 2015. The Drosophila bag of marbles
885 Gene Interacts Genetically with Wolbachia and Shows Female-Specific Effects of
886 Divergence. PLoS Genet. 11(8). doi:10.1371/journal.pgen.1005453.

887 Flores HA, DuMont VLB, Fatoo A, Hubbard D, Hijji M, Barbash DA, Aquadro CF. 2015.
888 Adaptive evolution of genes involved in the regulation of germline stem cells in
889 Drosophila melanogaster and D. simulans. G3 Genes, Genomes, Genet. 5(4):583–
890 592. doi:10.1534/g3.114.015875.
891 Gleason RJ, Anand A, Kai T, Chen X. 2018. Protecting and diversifying the germline.
892 Genetics. 208(2):435–471. doi:10.1534/genetics.117.300208.
893 Glover DM, Raff J, Karr TL, O'Neill SL, Lin H, Wolfner MF. 1990. Parasites in
894 Drosophila embryos. Nature. 348:117. doi:10.1038/348117a0.
895 Gönczy P, Matunis E, DiNardo S. 1997. bag-of-marbles and benign genial cell
896 neoplasm act in the germline to restrict proliferation during Drosophila
897 spermatogenesis. Development. 124(21):4361–4371.
898 doi:10.1242/dev.124.21.4361.
899 Gonzalez J, Qi H, Liu N, Lin H. 2015. Piwi Is a Key Regulator of Both Somatic and
900 Germline Stem Cells in the Drosophila Testis. Cell Rep. 12(1):150–161.
901 doi:10.1016/J.CELREP.2015.06.004.
902 Gratz SJ, Ukken FP, Rubinstein CD, Thiede G, Donohue LK, Cummings AM, Oconnor-
903 Giles KM. 2014. Highly specific and efficient CRISPR/Cas9-catalyzed homology-
904 directed repair in Drosophila. Genetics. 196(4):961–971.
905 doi:10.1534/genetics.113.160713.
906 Gubala AM, Schmitz JF, Kearns MJ, Vinh TT, Bornberg-Bauer E, Wolfner MF, Findlay
907 GD. 2017. The Goddard and Saturn Genes Are Essential for Drosophila Male
908 Fertility and May Have Arisen de Novo. Mol Biol Evol. doi:10.1093/molbev/msx057.
909 Hinnant TD, Merkle JA, Ables ET. 2020. Coordinating Proliferation, Polarity, and Cell
910 Fate in the Drosophila Female Germline. Front Cell Dev Biol. 8:19.
911 doi:10.3389/fcell.2020.00019.
912 Ho J, Tumkaya T, Aryal S, Choi H, Claridge-Chang A. 2019. Moving beyond P values:
913 data analysis with estimation graphics. Nat Methods. 16(7):565–566.
914 doi:10.1038/s41592-019-0470-3.
915 Howe KL, Contreras-Moreira B, De Silva N, Maslen G, Akanni W, Allen J, Alvarez-
916 Jarreta J, Barba M, Bolser DM, Cambell L, et al. 2020. Ensembl Genomes 2020-
917 enabling non-vertebrate genomic research. Nucleic Acids Res. 48(D1).

918 doi:10.1093/nar/gkz890.
919 Insco ML, Bailey AS, Kim J, Olivares GH, Wapinski OL, Tam CH, Fuller MT. 2012. A
920 self-limiting switch based on translational control regulates the transition from
921 proliferation to differentiation in an adult stem cell lineage. Cell Stem Cell.
922 11(5):689–700. doi:10.1016/j.stem.2012.08.012.
923 Insco ML, Leon A, Tam CH, McKearin DM, Fuller MT. 2009. Accumulation of a
924 differentiation regulator specifies transit amplifying division number in an adult stem
925 cell lineage. Proc Natl Acad Sci. 106(52):22311–22316.
926 doi:10.1073/PNAS.0912454106.
927 Jenny A, Hachet O, Závorszky P, Cyrklaff A, Weston MDJ, St Johnston D, Erdélyi M,
928 Ephrussi A. 2006. A translation-independent role of oskar RNA in early Drosophila
929 oogenesis. Development. 133(15):2827–2833. doi:10.1242/dev.02456.
930 Jiang X, Assis R. 2017. Natural selection drives rapid functional evolution of young
931 drosophila duplicate genes. Mol Biol Evol. 34(12):3089–3098.
932 doi:10.1093/molbev/msx230.
933 Kaessmann H. 2010. Origins, evolution, and phenotypic impact of new genes. Genome
934 Res. 20(10):1313–1326. doi:10.1101/gr.101386.109.
935 Kahney EW, Snedeker JC, Chen X. 2019. Regulation of Drosophila germline stem cells.
936 Curr Opin Cell Biol. 60:27–35. doi:10.1016/j.ceb.2019.03.008.
937 Kelleher ES, Jaweria J, Akoma U, Ortega L, Tang W. 2018. QTL mapping of natural
938 variation reveals that the developmental regulator bruno reduces tolerance to P-
939 element transposition in the Drosophila female germline. PLoS Biol. 16(10).
940 doi:10.1371/journal.pbio.2006040.
941 Klasberg S, Bitard-Feildel T, Callebaut I, Bornberg-Bauer E. 2018. Origins and
942 structural properties of novel and *de novo* protein domains during insect evolution.
943 FEBS J. 285(14):2605–2625. doi:10.1111/febs.14504.
944 Kriventseva E V., Kuznetsov D, Tegenfeldt F, Manni M, Dias R, Simão FA, Zdobnov
945 EM. 2019. OrthoDB v10: Sampling the diversity of animal, plant, fungal, protist,
946 bacterial and viral genomes for evolutionary and functional annotations of
947 orthologs. Nucleic Acids Res. 47(D1). doi:10.1093/nar/gky1053.
948 Lack JB, Cardeno CM, Crepeau MW, Taylor W, Corbett-Detig RB, Stevens KA, Langley

949 CH, Pool JE. 2015. The drosophila genome nexus: A population genomic resource
950 of 623 Drosophila melanogaster genomes, including 197 from a single ancestral
951 range population. Genetics. doi:10.1534/genetics.115.174664.
952 Lavoie CA, Ohlstein B, McKearin DM. 1999. Localization and function of bam protein
953 require the benign gonial cell neoplasm gene product. Dev Biol.
954 doi:10.1006/dbio.1999.9346.
955 Levine MT, Jones CD, Kern AD, Lindfors HA, Begun DJ. 2006. Novel genes derived
956 from noncoding DNA in Drosophila melanogaster are frequently X-linked and
957 exhibit testis-biased expression. National Academy of Sciences.
958 Li F, Rane R V, Luria | Victor, Xiong Z, Chen J, Li Z, Catullo RA, Griffin PC, Schiffer M,
959 Pearce S, et al. 2021. Phylogenomic analyses of the genus Drosophila reveals
960 genomic signals of climate adaptation. Mol Ecol Resour. 00:1–23.
961 doi:10.1111/1755-0998.13561.
962 Li Y, Minor NT, Park JK, McKearin DM, Maines JZ. 2009. Bam and Bgcn antagonize
963 Nanos-dependent germ-line stem cell maintenance. Proc Natl Acad Sci U S A.
964 106(23):9304–9309. doi:10.1073/pnas.0901452106.
965 Markow TA, O'Grady P. 2006. Drosophila: A Guide to Species Identification and Use.
966 Elsevier Science.
967 McKearin DM, Spradling AC. 1990. Bag-of-marbles: A Drosophila gene required to
968 initiate both male and female gametogenesis. Genes Dev. 4(12 B):2242–2251.
969 doi:10.1101/gad.4.12b.2242.
970 Messer PW, Petrov DA. 2013. Frequent adaptation and the McDonald-Kreitman test.
971 Proc Natl Acad Sci U S A. 110(21):8615–8620. doi:10.1073/pnas.1220835110.
972 Mou H, Smith JL, Peng L, Yin H, Moore J, Zhang XO, Song CQ, Sheel A, Wu Q, Ozata
973 DM, et al. 2017. CRISPR/Cas9-mediated genome editing induces exon skipping by
974 alternative splicing or exon deletion. Genome Biol. 18(1):108. doi:10.1186/s13059-
975 017-1237-8.
976 Pereverzev AP, Gurskaya NG, Ermakova G V., Kudryavtseva EI, Markina NM, Kotlobay
977 AA, Lukyanov SA, Zaraisky AG, Lukyanov KA. 2015. Method for quantitative
978 analysis of nonsense-mediated mRNA decay at the single cell level. Sci Rep.
979 5(1):1–10. doi:10.1038/srep07729.

980 Port F, Chen HM, Lee T, Bullock SL. 2014. Optimized CRISPR/Cas tools for efficient
981 germline and somatic genome engineering in Drosophila. Proc Natl Acad Sci U S
982 A. 111(29). doi:10.1073/pnas.1405500111.
983 Schaeffer SW, Miller EL. 1991. Nucleotide sequence analysis of Adh genes estimates
984 the time of geographic isolation of the Bogota population of Drosophila
985 pseudoobscura. Proc Natl Acad Sci U S A. 88(14):6097–6101.
986 doi:10.1073/pnas.88.14.6097.
987 Shivdasani AA, Ingham PW. 2003. Regulation of Stem Cell Maintenance and Transit
988 Amplifying Cell Proliferation by TGF-β Signaling in Drosophila Spermatogenesis.
989 Curr Biol. doi:10.1016/j.cub.2003.10.063.
990 Siddiq MA, Loehlin DW, Montooth KL, Thornton JW. 2017. Experimental test and
991 refutation of a classic case of molecular adaptation in Drosophila melanogaster.
992 Nat Ecol Evol. 1(2). doi:10.1038/s41559-016-0025.
993 Signor SA, New FN, Nuzhdin S. 2018. A large panel of drosophila simulans reveals an
994 abundance of common variants. Genome Biol Evol. doi:10.1093/gbe/evx262.
995 Simkin A, Wong A, Poh YP, Theurkauf WE, Jensen JD. 2013. Recurrent and recent
996 selective sweeps in the piRNA pathway. Evolution (N Y). 67(4):1081–1090.
997 doi:10.1111/evo.12011.
998 Sui T, Song Y, Liu Z, Chen M, Deng J, Xu Y, Lai L, Li Z. 2018. CRISPR-induced exon
999 skipping is dependent on premature termination codon mutations. Genome Biol.
1000 doi:10.1186/s13059-018-1532-z.
1001 Thurmond J, Goodman JL, Strelets VB, Attrill H, Gramates LS, Marygold SJ, Matthews
1002 BB, Millburn G, Antonazzo G, Trovisco V, et al. 2019. FlyBase 2.0: the next
1003 generation. Nucleic Acids Res. 47(D1):D759–D765. doi:10.1093/NAR/GKY1003.
1004 Ting X. 2013. Control of germline stem cell self-renewal and differentiation in the
1005 Drosophila ovary: Concerted actions of niche signals and intrinsic factors. Wiley
1006 Interdiscip Rev Dev Biol. 2(2):261–273. doi:10.1002/wdev.60.
1007 True JR, Haag ES. 2001. Developmental system drift and flexibility in evolutionary
1008 trajectories. Evol Dev. 3(2):109–119. doi:10.1046/j.1525-142X.2001.003002109.x.
1009 Turissini DA, Liu G, David JR, Matute DR. 2015. The evolution of reproductive isolation
1010 in the Drosophila yakuba complex of species. J Evol Biol. 28(3):557–575.

1011 doi:10.1111/jeb.12588.
1012 Turissini DA, Matute DR. 2017. Fine scale mapping of genomic introgressions within the
1013 Drosophila yakuba clade. PLoS Genet. 13(9). doi:10.1371/journal.pgen.1006971.
1014 Vakirlis N, McLysaght A. 2019. Computational Prediction of De Novo Emerged Protein-
1015 Coding Genes. In: Methods in Molecular Biology. Vol. 1851. Humana Press Inc. p.
1016 63–81.
1017 Wilson BA, Foy SG, Neme R, Masel J. 2017. Young genes are highly disordered as
1018 predicted by the preadaptation hypothesis of de novo gene birth. Nat Ecol Evol.
1019 1(6). doi:10.1038/s41559-017-0146.
1020 Witt E, Benjamin S, Svetec N, Zhao L. 2019. Testis single-cell RNA-seq reveals the
1021 dynamics of de novo gene transcription and germline mutational bias in drosophila.
1022 Elife. doi:10.7554/eLife.47138.
1023 Yang Z. 1997. Paml: A program package for phylogenetic analysis by maximum
1024 likelihood. Bioinformatics. doi:10.1093/bioinformatics/13.5.555.
1025 Yang Z. 2007. PAML 4: Phylogenetic analysis by maximum likelihood. Mol Biol Evol.
1026 doi:10.1093/molbev/msm088.
1027 Zhai W, Nielsen R, Slatkin M. 2009. An investigation of the statistical power of neutrality
1028 tests based on comparative and population genetic data. Mol Biol Evol. 26(2).
1029 doi:10.1093/molbev/msn231.
1030 Zhou Q, Zhang G, Zhang Y, Xu S, Zhao R, Zhan Z, Li X, Ding Y, Yang S, Wang W.
1031 2008. On the origin of new genes in Drosophila. Genome Res. 18(9):1446–1455.
1032 doi:10.1101/gr.076588.108.
1033

Fig 1. Species chosen to generate *bam* null alleles using CRISPR/Cas9 to disrupt *bam* with a trackable eye marker cassette. (A) The five species we chose to generate *bam* null alleles span approximately 30 million years of divergence. (B) Schematic for generating null alleles with trackable eye markers using CRISPR/Cas9. We generate two null alleles using different color eye markers and cross the heterozygotes together to generate an easily trackable null genotype.

Fig 2. *Bam* is necessary for female and male fertility in *D. melanogaster, D. simulans, and D. yakuba,* but not for *D. ananassae* males nor both *D. teissieri* males and females. Swarm plots showing the total progeny per female or per male for each *bam* genotype and Cumming estimation plots showing the 95% confidence interval effect size. Dotted boxes show genotypes where the phenotype did not match that of *D. melanogaster.* For *D. melanogaster, D. simulans, and D. yakuba*, the *bam* null DsRed/YFP females and males were sterile ($P < 0.0001$, permutation test), and the heterozygous genotypes did not have a significant effect on fertility ($P > 0.05$, permutation test). For *D. teissieri,* the *bam* null DsRed/YFP females and males did not have significantly different fertility from wildtype, nor did the heterozygotes. For *D. ananassae*, the *bam* null DsRed/YFP females were sterile ($P < 0.0001$, permutation test), and the heterozygotes did not affect fertility. However, the *bam* null DsRed/YFP males were fertile and there was no significant difference between the null and heterozygotes and wildtype fertility ($P>0.05$, permutation test).

Fig 3. *Bam* is necessary for female and male germline stem cell differentiation in *D. melanogaster, D. simulans, and D. yakuba,* but not for *D. ananassae* males nor *D. teissieri* males and females. (A) Schematics of ovaries and testes showing the *bam* wildtype and null cytological phenotypes in *D. melanogaster*. Wildtype *bam* ovaries exhibit developing egg chambers with differentiated nurse cells and testes exhibit large, differentiated spermatocytes. Null *bam* ovaries exhibit egg chambers filled with small GSC-like tumors that contain undeveloped fusomes and testes exhibit cysts filled with small over-proliferating spermatogonia. (B) Ovaries and testes from all five species of

wildtype (*bam*$^{+}$/*bam*$^{+}$*),* heterozygous (YFP/+ or DsRed/+)*,* and null (DsRed/YFP) *bam* genotypes. All tissue is labeled with antibodies to Vasa (germline) and Hts-1B1 (fusome). Dashed boxes indicate genotypes and tissue that are not consistent with the *D. melanogaster* phenotype. Ovaries and testes from all five species exhibit developing nurse cells or spermatocytes (respectively) for wildtype and heterozygous *bam* genotypes. We did not observe any tumorous cysts (arrowheads). Ovaries and testes from *bam* null *D. melanogaster, D. simulans, and D. yakuba* all exhibited cysts filled with GSC-like tumors (ovaries) or over-proliferating spermatogonia (testes) (arrows). The *bam* null ovaries exhibit undeveloped fusomes. *D. ananassae bam* null ovaries exhibited the tumorous egg chamber phenotype (arrow), however testes exhibited large developing spermatocytes (arrowhead) and we did not observe any tumors. The *bam* null *D. teissieri* ovaries and testes exhibited nurse cell positive egg chambers and developing spermatocytes (respectively) (arrowheads) and we did not observe any tumors.

Fig 4. Loss of *bam* function in *D. ananassae* males shows ectopic expression of Fas3, a marker expressed in the hub, but not in *D. teissieri*. All testes tissue is labeled with antibodies for Vasa (germline) and Fas3 (hub, arrowheads). Significance was assessed with a Fisher's exact test comparing counts of testes with ectopic Fas3 expression between wildtype and *bam* null testes. (A) *D. melanogaster bam* wildtype testes with Fas3 expression limited to the anterior tip of the testes hub (inset) and featuring large differentiating spermatogonia (Fas3 ectopic expression n=0/13). (B) *D. melanogaster bam* null testes feature ectopic Fas3 expression and small over-proliferating spermatogonia (Fas3 ectopic expression n=8/11, P<0.000). (C) *D. teissieri bam* wildtype testes with Fas3 expression limited to the anterior tip of the testes (hub) and featuring large differentiating spermatogonia (Fas3 ectopic expression n=0/20). (D) *D. teissieri bam* null testes with Fas3 expression limited to the anterior tip of the testes (hub) and large differentiating spermatogonia (Fas3 ectopic expression n=0/16, P=1). (E) *D. ananassae bam* wildtype testes with Fas3 expression limited to the hub and featuring large differentiating spermatogonia (Fas3 ectopic expression n=31). (F) *D. ananassae bam* null

testes with ectopic Fas3 expression and large differentiating spermatogonia (Fas3 ectopic expression n=19/27, P<0.000).

Fig 5. *Bam* shows lineage-specific signals of positive selection scattered across the *Drosophila* genus. Cladogram of *Drosophila* species we sampled in this study. Pink highlighted lineages represent lineages where we have evidence of positive selection at *bam* with the McDonald Kreitman test. Blue highlighted lineages are lineages of which we could not reject neutrality with the McDonald Kreitman test. The 2X2 table from the McDonald Kreitman test is shown on the right (N = nonsynonymous, S = synonymous). Alpha is the proportion of nonsynonymous fixations predicted to be due to positive selection. P-value is from the Chi-square test, n is sample size.

[1]Polymorphism data from Choi and Aquadro 2014.

Fig S1. RT-qPCR experiment to assess *bam* mRNA in *D. ananassae bam* null genotypes reported as the relative quantity (RQ) of *bam* expression to the housekeeping control RP49. *bam* expression in testes of the null (DsRed/YFP) genotype is significantly reduced (standard error) relative to *bam* expression in testes of the wildtype genotype at approximately 10%, consistent with expectations for NMD. The heterozygous genotypes DsRed/+ and YFP/+ do not show reduced *bam* expression relative to wildtype.

Fig S2. RT-qPCR experiment to detect patterns consistent with nonsense mediated mRNA decay of the *bam* disruption allele in *D. teissieri* reported as the relative quantity (RQ) of mRNA from the *bam* disruption allele to the *bam* wildtype allele in heterozygotes. Significance reported as standard error (A) Expression of the *bam* null allele relative to the *bam* wildtype allele in ovaries. Both heterozygous genotypes DsRed/+ and YFP/+ show less than 10% of expression of the *bam* null allele

relative to the wildtype allele, consistent with expectations for NMD. The wildtype negative control shows little to no expression of the null allele as expected. (B) Expression of the *bam* null allele relative to the *bam* wildtype allele in testes. Both heterozygous genotypes DsRed/+ and YFP/+ show less than 50% of expression of the *bam* null allele relative to the wildtype allele, consistent with expectations for NMD. The wildtype negative control shows little to no expression of the null allele as expected.

Fig S3. RT-qPCR experiment to detect evidence of exon skipping of the exon containing the *bam* disruption reported as the relative quantity (RQ) of *bam* exon 1 to exon 2. Significance reported as standard error (A) Expression of *bam* exon 1 relative to exon 2 in ovaries. The RQ of exon 1 to exon 2 in the *bam* null DsRed/YFP genotype is not significantly different than the RQ of exon 1 to exon 2 in the *bam* wildtype genotype, indicating that expression of the exon containing the disruption is comparable to the unaffected exon in both the null and wildtype genotype, and therefore exon skipping is not likely occurring in females. (B) Expression of *bam* exon 1 relative to exon 2 in testes. The RQ of exon 1 to exon 2 in the *bam* null DsRed/YFP genotype is not significantly different than the RQ of exon 1 to exon 2 in the *bam* wildtype genotype, indicating that expression of the exon containing the disruption is comparable to the unaffected exon in both the null and wildtype genotype, and therefore exon skipping is not likely occurring in males.

Table 1. Abbreviations for *bam* genotypes for all species and the expected phenotypes as observed in *D. melanogaster*.

		***D. melanogaster* Phenotype Expectations**		
Genotype	**Abbreviation**	**Eye Color**	**Fertility**	**Cytological**
bam^{+}/bam^{+}	wildtype	white	wildtype	wildtype
$bam^{3xP3\text{-}DsRed}/bam^{+}$	DsRed/+	DsRed	wildtype	wildtype
$bam^{3xP3\text{-}YFP}/bam^{+}$	YFP/+	YFP	wildtype	wildtype
$bam^{3xP3\text{-}DsRed}/bam^{3xP3\text{-}YFP}$	DsRed/YFP	DsRed & YFP	sterile	tumorous ovaries and testes

Fig1

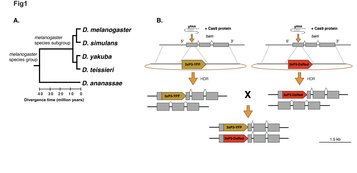

Fig2

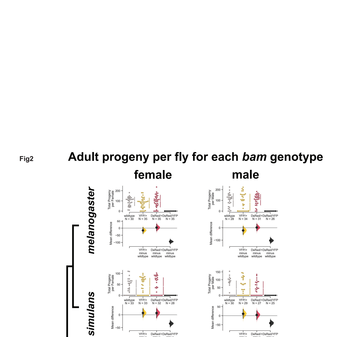

Fig3

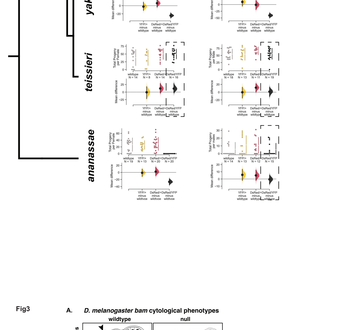

Fig4

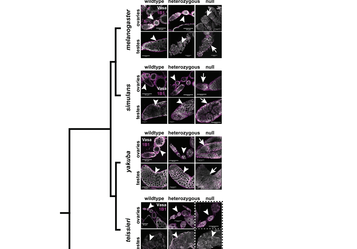

Fig5

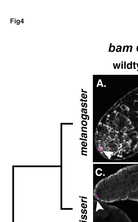

	Dn	Ds	Pn	Ps	alpha	P-value	n
D. melanogaster	33	13	1	7	**0.943**	***0.001***	187
D. simulans	34	17	5	9	**0.722**	***0.036***	20
D. yakuba	26	18	2	13	**0.893**	***0.002***	14
D. santomea	24	23	1	4	0.76	0.186	11
D. teissieri	11	13	9	9	-0.181	0.789	11
D. serrata	61	52	4	17	**0.799**	***0.003***	18
D. burnanda	67	45	3	1	-1.014	0.542	20
D. birchii	40	39	13	39	**0.675**	***0.003***	20
D. jambulina	59	45	10	20	**0.618**	***0.023***	19
D. bipectinata	23	14	18	17	0.355	0.357	20
D. pseudoananassae	30	28	2	1	-0.866	0.613	20
D. pandora	27	30	3	10	0.666	0.11	17
D. ananassae[1]	28	33	0	5	**1**	***0.045***	14
D. pseudoobscura	39	40	2	4	0.487	0.448	11
D. affinis	31	32	2	1	-1.064	0.349	14
D. mojavensis	2	5	2	7	0.285	0.771	22
D. immigrans	60	53	3	3	0.116	0.882	20
D. rubida	75	73	0	14	**1**	***0.000***	19

Fig S1

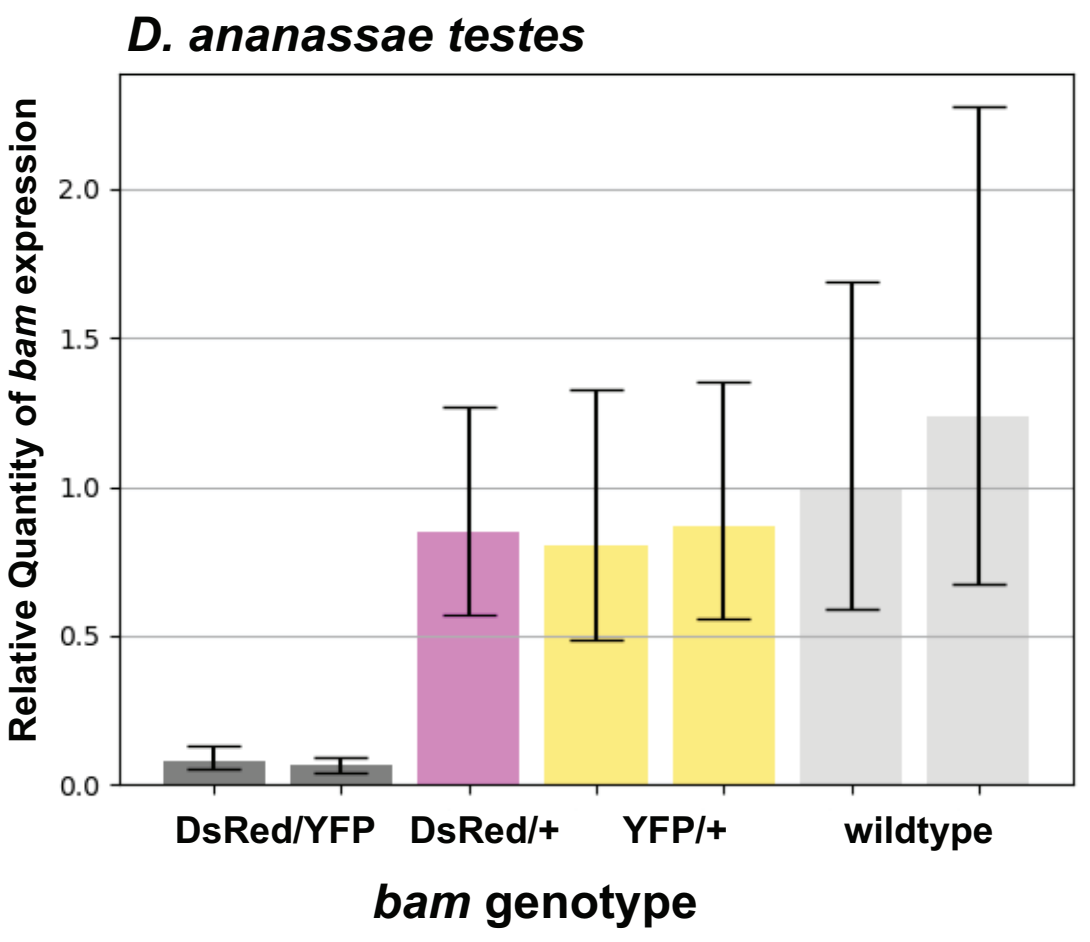

Fig S2

A. *D. teissieri* ovaries

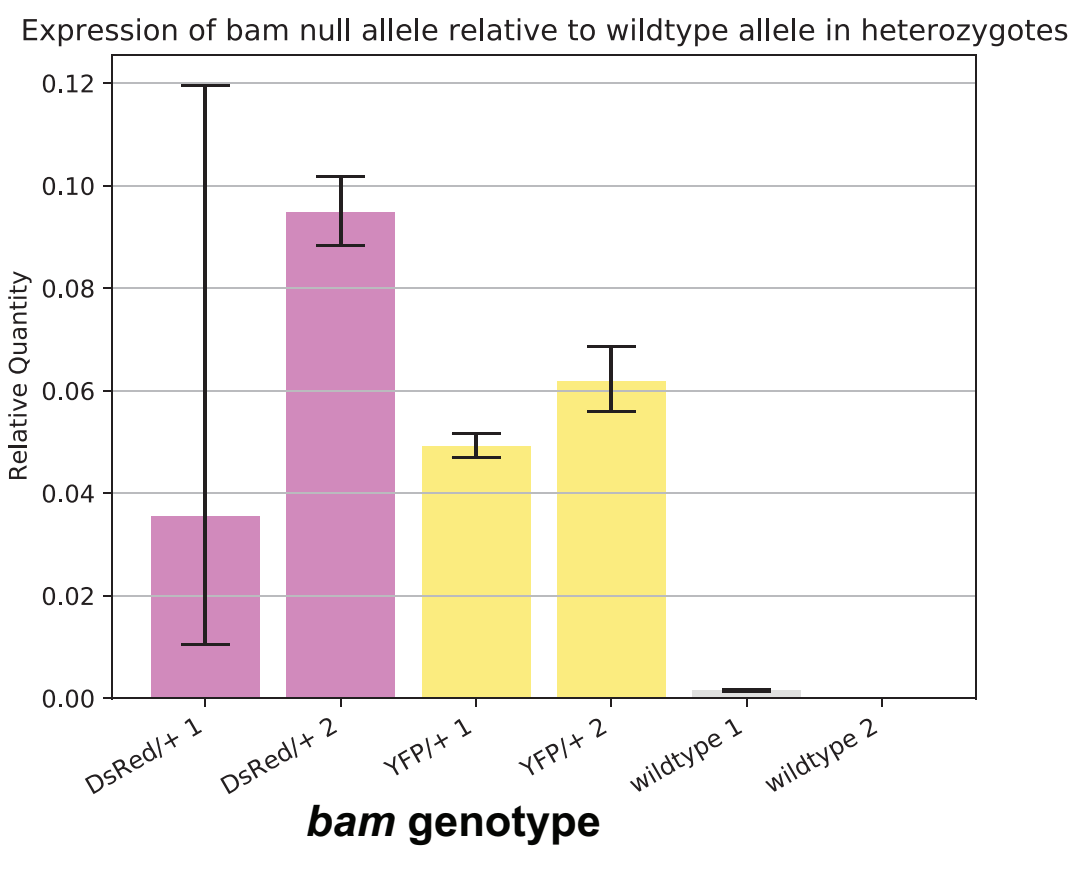

B. *D. teissieri* testes

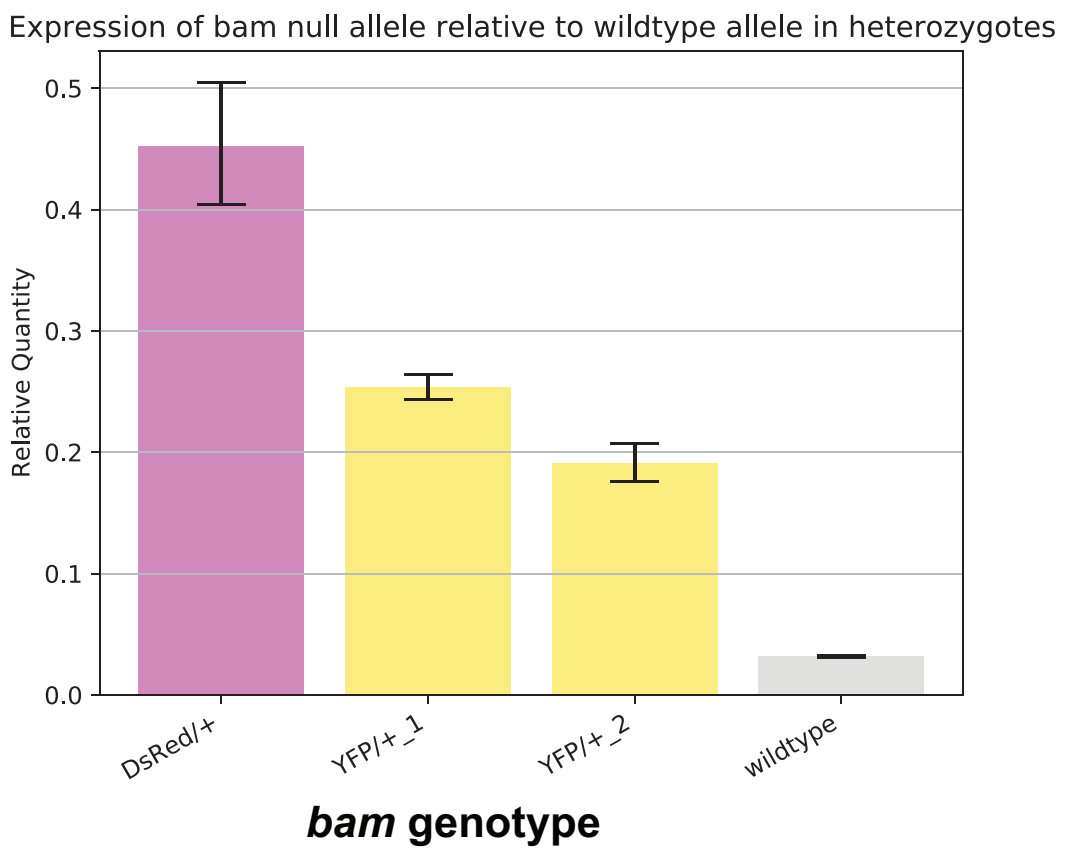

Fig S3

A. *D. teissieri* ovaries

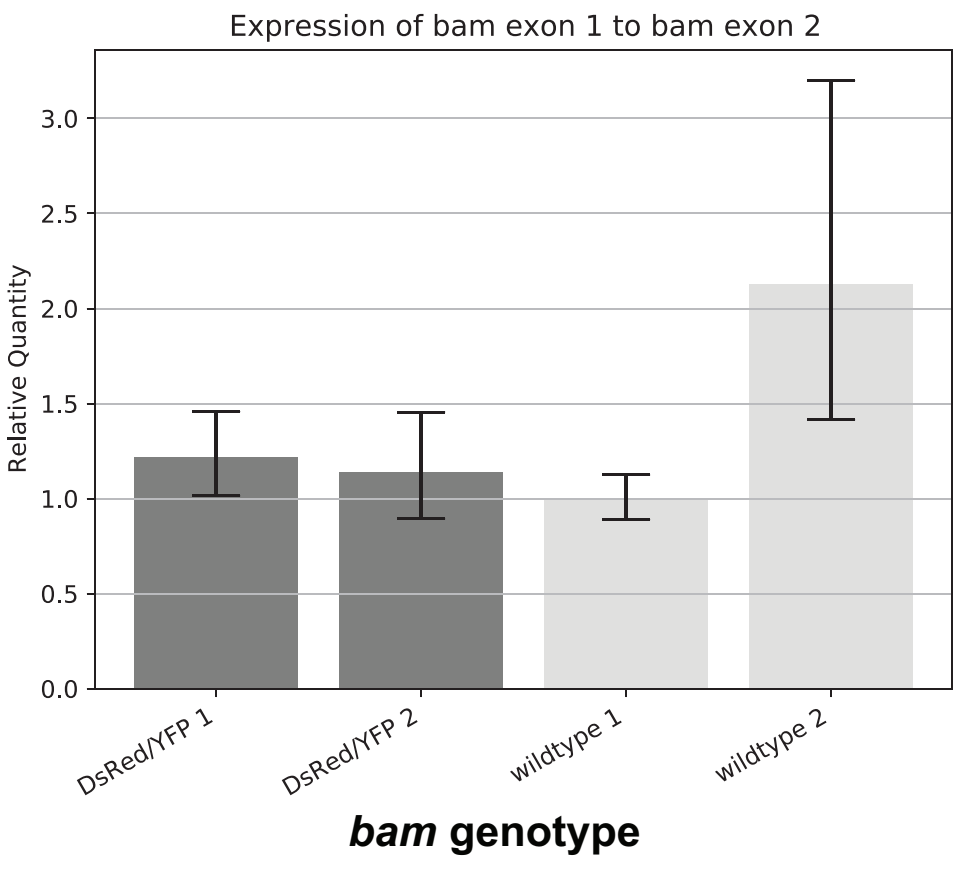
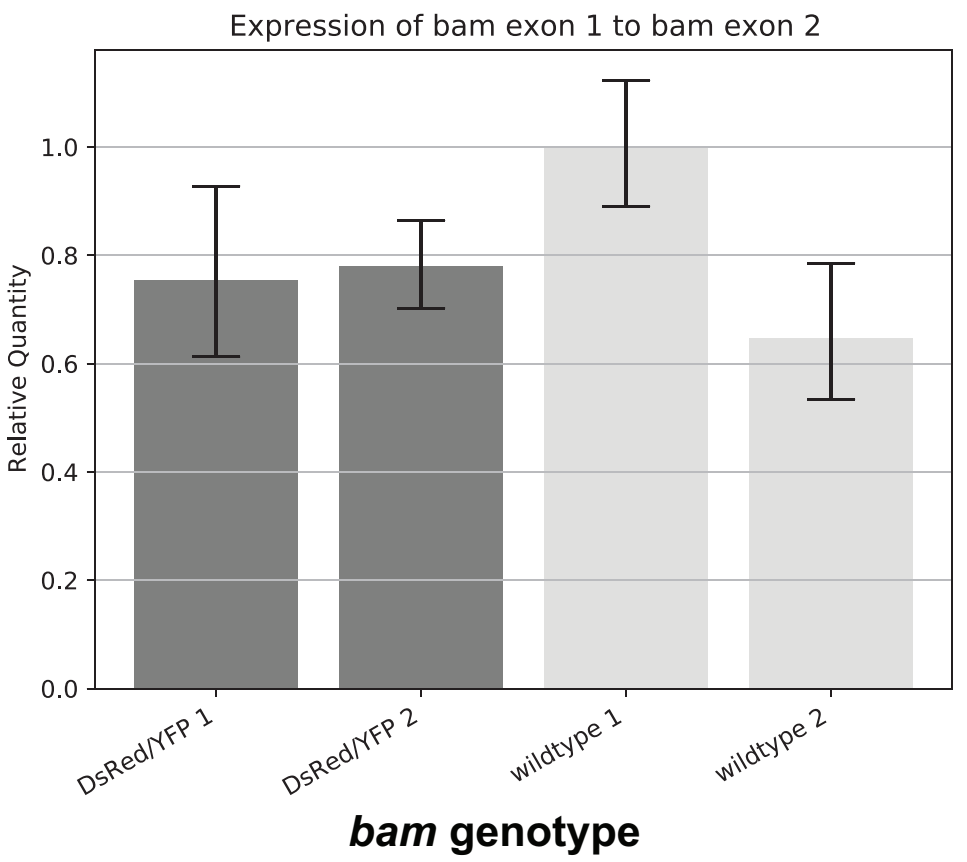
B. *D. teissieri* testes